Theoretical study for a quantum-dot molecule irradiated by a microwave field

Qing-feng Sun
Department of Physics, The University of Hong Kong, Pokfulam Road, Hong Kong, China
and Department of Physics, Peking University, Beijing 100871, China

Jian Wang
Department of Physics, The University of Hong Kong, Pokfulam Road, Hong Kong, China

Tsung-han Lin
Department of Physics, The University of Hong Kong, Pokfulam Road, Hong Kong, China
and Department of Physics, Peking University, Beijing 100871, China
(Received 20 December 1999)

Motivated by the recent experiment by Oosterkamp *et al.* [Nature **395**, 873 (1998)] we have developed a theory to describe electron tunneling through two coupled quantum dots irradiated by a microwave field. Our results for both the weak- and strong-coupling regimes are in excellent agreement with experiment. In addition, our theory suggests several unique features in the strong-coupling regime, including Rabi oscillations, which can be verified experimentally. The main resonance and the sideband resonance of the molecular level are also calculated for the entire range of the coupling strength, and show interesting crossover behavior.

Tunneling phenomena through two coupled quantum dots have received much attention in recent years.[1–5] Compared to the single quantum-dot system, the quantum-dot molecule has much richer physics. When the coupling is weak, the electrons are basically localized on individual dots, the two coupled dots form an ''ionic molecule.''[1] On the contrary, when the coupling between the two dots is strong, the electrons are delocalized over both dots to form a ''covalent molecule.''

Recently, Oosterkamp *et al.*[1] investigated the microwave (MW) spectroscopy of a two-coupled quantum-dot molecule connected to two contacts. They demonstrated that the two dots can be coupled into an artificial molecule in a coherent way, and found the following features: (1) For the weak-coupling case, the well-known photon-assisted (PA) resonances occur if $\Delta E = \pm n\hbar\omega$ $(n=1,2,\ldots)$, where ΔE is the energy difference between the two uncoupled levels of the two dots, and ω is the frequency of the MW field; the heights of the PA resonance peaks are proportional to $J_n^2(\alpha)$, where $J_n(\alpha)$ is the nth-order Bessel function, $\alpha = eV_{ac}/\hbar\omega$, and V_{ac} is the MW amplitude. (2) For the strong-coupling case, the locations of the PA resonance peaks change significantly, appearing at $\hbar\omega = \tilde{\epsilon} \equiv \sqrt{\Delta E^2 + 4T^2}$, where T is the tunneling strength between the two dots.[1]

Theoretically, the ionic molecule irradiated by a MW field has already been studied,[6,7] but the covalent molecule has received less attention.[8] The theory presented in the present paper covers the whole range of coupling strength, and can be used to study the weak- and strong-coupling cases as well as the crossover between them. In contrast to Ref. 8, which can only be applied to the high bias case, this work has no restriction on the bias voltage, so that it can be used to study zero bias as well as high bias transport under the irradiation of the MW field. The system we considered consists of two-coupled quantum dots irradiated by a MW field, connected to two external contacts. We assume that the electron tunneling through the quantum-dot molecule is coherent and that only one electronic state in each dot is involved, both facts consistent with the experiment. By using the nonequilibrium Green-function method, we obtain an analytical solution for the average current and find the following (1) The locations of the PA resonance peaks are in excellent agreement with the experiment[1] for both the weak- and strong-coupling cases. (2) The heights of the PA resonance peaks are proportional to $J_n^2(\alpha)$ for the weak-coupling case, which agrees well with the experiment[1] and with previous work.[6,9] However, for the strong-coupling case, the heights rise much faster than $J_n^2(\alpha)$, a result not reported in the experiment. (3) For the strong-coupling case, the argument of the Bessel functions in the current formula, α, is equal to $eV_{ac}\Delta E/\omega\tilde{\epsilon}$, a value different from that in previous studies where $\alpha = eV_{ac}/\omega$.[6,7,9,10] This leads to the suppression of the sideband resonance of the molecular level in the strong-coupling limit. (4) In the weak-coupling case, Stafford and Wingreen found that the PA resonant peak is split into two peaks due to Rabi oscillations.[6,11,12] In the strong-coupling case, we find that additional splitting occurs as a result of higher-order virtual processes. (5) As the coupling strength is varied, the system shows an interesting crossover from the covalent molecule states to the ionic molecule states.

The quantum-dot molecule is modeled by the following Hamiltonian:

$$H = \sum_{k,\beta\in l,r} \epsilon_{k\beta} a_{k\beta}^{\dagger} a_{k\beta} + \sum_{\beta\in l,r} \epsilon_{\beta}(t) c_{\beta}^{\dagger} c_{\beta} + [\,T c_l^{\dagger} c_r + \text{H.c.}] + \sum_{k,\beta\in l,r} (v_{k\beta} a_{k\beta}^{\dagger} c_{\beta} + \text{H.c.}), \quad (1)$$

where $a_{k\beta}^{\dagger}$ is the creation operator for electrons in the lead-β, $c_{\beta}^{\dagger}$ is the creation operator for electrons in the dot β, and

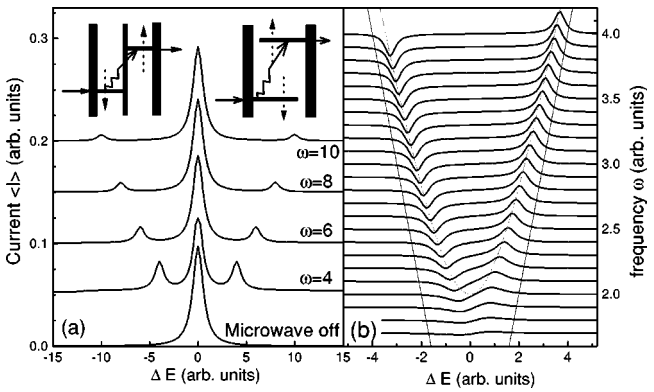

FIG. 1. The averaged current $\langle I\rangle$ vs ΔE for different frequencies ω. (a) The weak-coupling case with $\Gamma=0.5$, $T=0.2$, $V_{ac}=4$, and $\mu_L=-\mu_R=10$. Different curves have been offset by 0.05 along the vertical axis for clarity. The insets are schematic diagrams for the two-coupled dots irradiated by a MW field. The left inset is the uncoupled energy levels of the two dots. The right is the two levels of the quantum-dot molecule. (b) The strong-coupling case with $\Gamma=0.1$, $T=1$, $V_{ac}/\omega=0.2$, and $\mu_L=\mu_R=0$. Different curves in (b) have been offset such that the right vertical axis gives the frequency.

T is the interdot coupling. Considering the experimental setup, we assume that the MW field irradiates only on the two dots, and induces an adiabatic change for the energy of each dot by[6,13,14]: $\epsilon_\beta(t)=\epsilon_\beta^0\pm(eV_{ac}/2)\cos\omega t$, where $+$ and $-$ correspond to the left and the right dot, respectively.

To proceed, we first perform a unitary transformation to diagonalize the Hamiltonian in the absence of the MW field such that the transformed Hamiltonian is written as $H=H_0+H_I$, with

$$H_0=\sum_{k,\beta}\epsilon_{k\beta}a_{k\beta}^\dagger a_{k\beta}+\sum_{i=1,2}\left[\frac{\tilde\epsilon}{2}-\frac{eV_{ac}\Delta E\cos\omega t}{2\tilde\epsilon}\right](-)^i\tilde c_i^\dagger\tilde c_i$$
$$+\sum_{k,i=1,2}\frac{1}{\sqrt{2}}\{v_{kl}\tilde v_{li}a_{kl}^\dagger\tilde c_i+v_{kr}\tilde v_{ri}a_{kr}^\dagger\tilde c_i+\text{H.c}\},\qquad(2)$$

$$H_I=2\gamma\cos\omega t[\tilde c_1^\dagger\tilde c_2+\tilde c_2^\dagger\tilde c_1],\qquad(3)$$

where $\gamma=eV_{ac}T/2\tilde\epsilon$, $\tilde v_{li}=\sqrt{1-(-)^i\Delta E/\tilde\epsilon}$, $\tilde v_{ri}=(-1)^i\sqrt{1+(-)^i\Delta E/\tilde\epsilon}$, and we have set the zero point of the energy by assuming $\epsilon_r^0+\epsilon_l^0=0$. From Eqs. (2) and (3) we see that the MW field causes (1) two molecular levels varying simultaneously but out phase [the second term in Eq. (2)], this differs from the case of a single quantum dot with multilevels in which levels vary simultaneously and in phase;[15] (2) a new term appears in the Hamiltonian [Eq. (3)], leading to a direct transition between the two molecular levels [see the right inset of Fig. 1(a)].

The time-dependent particle current from the left lead can be expressed as ($\hbar=e=1$) (Ref. 13)

$$J_L(t)=-2\int_{-\infty}^t dt_1\int\frac{d\epsilon}{2\pi}\text{Im Tr}\{e^{-i\epsilon(t_1-t)}\mathbf{\Gamma}^L[\mathbf{G}^<(t,t_1)$$
$$+f_L(\epsilon)\mathbf{G}^r(t,t_1)]\},\qquad(4)$$

where the 2×2 matrix Green functions $\mathbf{G}^r$ and $\mathbf{G}^<$ are defined in the usual manner and $\mathbf{\Gamma}^L$ is the matrix linewidth function with $\mathbf{\Gamma}_{ij}^{L(R)}=\tilde v_{l(r)i}\tilde v_{l(r)j}\Gamma/2$. Here Γ is the linewidth function for the symmetric system in the absence of the MW field and is independent of energy in the wide-bandwidth approximation.[16,14]

The Green functions $\mathbf{G}^r$ and $\mathbf{G}^<$ can be obtained in the following way: find the Green functions $\mathbf{g}^r$ and $\mathbf{g}^<$ of H_0 using the fact that $\tilde c_1$ and $\tilde c_2$ are decoupled in H_0, then determine the Green functions $\mathbf{G}^r$ and $\mathbf{G}^<$ using the Dyson equation and the Keldysh equation. In this way, the Green function can be obtained analytically. For example, the retarded Green function $\mathbf{G}_{nm}^r(\epsilon)$ [Fourier transform of $G^r(t,t_1)$ (Ref. 17)] is given by[18]

$$G_{ii,nm}^r(\epsilon)=\sum_{k,k_1}\frac{\gamma J_{k+n}(\pm\alpha/2)X_{k-k_1}(\pm\alpha)J_{k_1+m}(\mp\alpha/2)}{\epsilon_k^\pm\epsilon_{k_1}^\mp-\gamma^2X_{k-k_1}^2(\alpha)},$$

$$G_{ii,nm}^r(\epsilon)=\sum_k\frac{J_{k+n}(\pm\alpha/2)J_{k+m}(\pm\alpha/2)}{\epsilon_k^\pm-\gamma^2\sum_{k_1}X_{k-k_1}^2(\alpha)/\epsilon_{k_1}^\mp},\qquad(5)$$

where $\epsilon_l^\pm\equiv\epsilon\pm\tilde\epsilon/2-l\omega+i\Gamma/2$, $X_l(\alpha)\equiv J_{l+1}(\alpha)+J_{l-1}(\alpha)$, $\alpha\equiv eV_{ac}\Delta E/\omega\tilde\epsilon$. Both $i,\bar i=1$ or 2, with $\bar i\neq i$. The upper and lower signs correspond to $i=1$ and 2, respectively.

Finally the time-averaged current is

$$\langle I\rangle=-\int\frac{d\epsilon}{2\pi}\text{Im Tr}\,\mathbf{\Gamma}^L[\mathbf{G}_{00}^<(\epsilon)+2f_L(\epsilon)\mathbf{G}_{00}^r(\epsilon)],\qquad(6)$$

where the index ''00'' represents a Fourier index of the matrix Green function. Equation (6) is valid for any interdot coupling strength. Notice that in this work the argument of the Bessel function α, which is equal to $eV_{ac}\Delta E/\omega\tilde\epsilon$, is different from that in previous works discussing the weak-coupling case or the single-dot system,[6,9,10] where $\alpha=eV_{ac}/\omega$. In the weak-coupling case, our results reproduce the previous ones. But for the strong-coupling case, it is significantly different from the weak-coupling case.

In the following we first discuss two extreme cases: the weak- and strong-coupling cases, and then the crossover between them, at zero temperature.

(1) The weak-coupling case ($2T\ll\Delta E$). In this regime, in the absence of a MW field, the two molecular states of this ionic molecule are basically localized in individual dots so that the molecular level spacing is approximately ΔE. The hopping elements between the molecular level to the left and right leads are highly asymmetric. However, in the presence of a MW field, if the photon energy is equal to the energy difference between two molecular levels, then an electron can tunnel from one dot to the other by emitting or absorbing a photon. Figure 1(a) shows the calculated averaged current vs ΔE for different MW frequencies ω when the bias voltage $V=\mu_L-\mu_R$ is much larger than both ω and ΔE. Two satellite resonance peaks emerge at $\Delta E=\pm\omega$. The separation between these satellites varies linearly with frequencies. When the two uncoupled levels are lined up (i.e., $\Delta E=0$), a high resonance emerges due to the main resonance. With the increase of the MW field, the multiple photon-assisted reso-

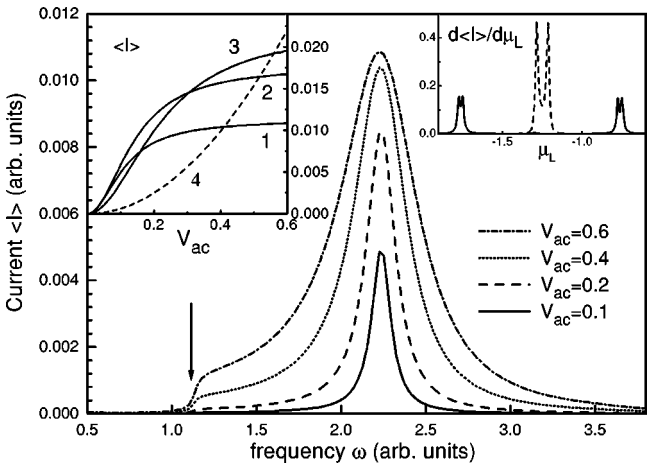

FIG. 2. The averaged current $\langle I\rangle$ vs the frequency ω at different MW amplitude V_{ac} with $\Gamma=0.05$, $T=1$, $\mu_L=\mu_R=0$, and $\Delta E=T$. The left inset shows the heights of the peaks at $\omega=\tilde{\epsilon}$ vs V_{ac} for different ΔE. Curves 1–3 correspond to $\Delta E=T$, $2T$, and $4T$, respectively. The curve 4 represents $J_1^2(\alpha)$, for comparison. The right inset shows $d\langle I\rangle/d\mu_L$ vs μ_L at the one-photon resonance $\omega=\tilde{\epsilon}$, where $\omega=2.5$, $\Gamma=0.02$, $V_{ac}=2.0$, and $\mu_R=0$. The dotted curve (with $T=0.1$ following $\Delta E\approx 2.49$) and the solid curve (with $\Delta E=0.1$ following $T\approx 1.249$) correspond to the weak- and strong-coupled cases.

nances will emerge at $\Delta E=\pm n\omega$ $(n=1,2,\ldots)$. The heights of the peaks are proportional to $J_n^2(\alpha)$ (not shown here). These results are in good agreement with the experiment by Oosterkamp *et al.* [Fig. 1(c) of Ref. 1].

(2) The strong-coupling case $(T\geqslant\Delta E)$. In this case, the two molecular states are delocalized over both dots to form a covalent molecule. In the presence of the MW field, we pay special attention to the zero-bias case as in the experiment,[1] in which the main resonance peak vanishes. Instead, only the current due to the photon-electron pumping effect occurs. Figure 1(b) shows the averaged photon-electron pumping current $\langle I\rangle$ vs ΔE for different frequencies. One sees that (1) when $\omega>2T$, a positive current peak appears at $\Delta E>0$, and a negative current peak at $\Delta E<0$. This can be understood as follows: when $\Delta E>0$, we have $\tilde{\epsilon}_1=-\tilde{\epsilon}/2$ and $\tilde{\epsilon}_2=\tilde{\epsilon}/2$ [see the right inset of Fig. 1(a)]. In this case, $\mathbf{\Gamma}_{11}^L>\mathbf{\Gamma}_{11}^R$. Hence an electron coming from the left lead (instead of the right lead) tunnels through the molecular level with energy $\tilde{\epsilon}_1$, absorbs a photon of energy $\omega=\tilde{\epsilon}$ to transit to the other molecular level with the energy $\tilde{\epsilon}_2$, then tunnels to the right lead resulting in a positive current peak (i.e., the electron flows from left to right). (2) The current peaks are not located at $\Delta E=\pm\omega$, but at $\pm\sqrt{\omega^2-(2T)^2}$, as shown by the dotted line in Fig. 1(b), where the solid line shows the weak-coupling case for comparison. This is because the molecular levels in the strong-coupling case are $\tilde{\epsilon}_1$ and $\tilde{\epsilon}_2$ so that the photon absorption condition is determined by $\omega=\tilde{\epsilon}$. (3) For $\omega<2T$, $\langle I\rangle$ nearly vanishes, due to the fact that the photon energy is lower than the energy difference of the two molecular levels for any ΔE. All the above-mentioned results are in excellent agreement with the experimental data of Oosterkamp *et al.* (Fig. 3(d) in Ref.1).

Figure 2 shows the pumping current $\langle I\rangle$ vs ω for different

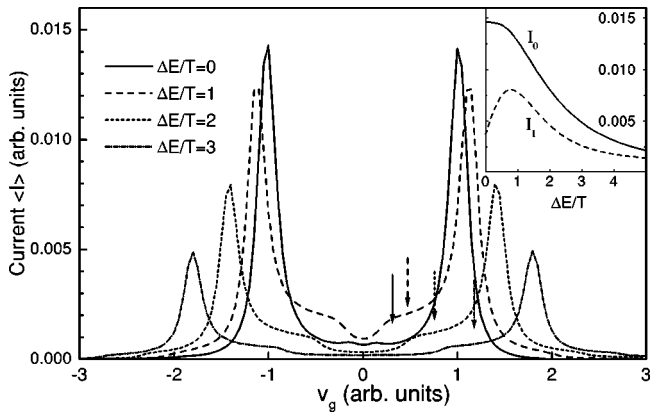

FIG. 3. $\langle I\rangle$ vs V_g at different $\Delta E/T$, showing the crossover from the strong-coupling to the weak-coupling regime, with $\omega=0.9$, $\Gamma=0.2$, $T=1$, $V_{ac}/\omega=0.6$, and $\mu_L=-\mu_R=0.05$. The inset shows the main resonance height I_0 at $V_g=\tilde{\epsilon}/2$ and the sideband resonance height I_1 at $V_g=\tilde{\epsilon}/2-\omega$ vs $\Delta E/T$, where we have multiplied I_1 by a factor of 5 for illustrating purposes.

MW amplitudes V_{ac}; this has not been reported experimentally. A peak emerges at the frequency $\omega=\tilde{\epsilon}$, corresponding to the photon-electron pumping effect. The half-width of the peak is determined by $\max\{\Gamma,\gamma\}$, not by Γ only. This result is quite different from the weak-coupling case in which the half-width is always determined by Γ at low temperature. The left inset in Fig. 2 shows the height of the peaks versus V_{ac} for different ΔE. In the weak-coupling case,[1,6,7] the height is proportional to the square of the Bessel function $J_1^2(\alpha)$ (dotted line). But in the strong-coupling case, the curve will deviate from $J_1^2(\alpha)$ since virtual processes like $J_0(\alpha)J_2(\alpha)$ will also contribute. At small α, the heights of the peaks rise much faster than $J_1^2(\alpha)$, because electrons tunnel back and forth frequently between the two dots inside the ''covalent molecule'' and dwell longer, leading to a significant increase of the probability for absorbing or emitting photons, hence a larger peak height. It would be interesting to check this result by further experiment. It should also be pointed out that near $\omega=\tilde{\epsilon}/2$ (the arrow in Fig. 2), the pumping current $\langle I\rangle$ drops to zero rapidly when ω decreases. This is because when $\omega<\tilde{\epsilon}/2$ an electron in the molecular level $-\tilde{\epsilon}/2$ cannot jump to any state of the lead by just absorbing a photon due to the Pauli exclusion principle.

(3) The crossover behavior. Figure 3 shows the current $\langle I\rangle$ vs the gate voltage V_g at small bias, in which we have set $V_g=V_{gl}=V_{gr}$,[19] and the gate voltage $V_{g\beta}$ $(\beta=l,r)$ controls the uncoupled intradot level by $\epsilon_\beta^0(V_{g\beta})=\epsilon_\beta^0(0)-eV_{g\beta}$. Notice that here we set $\omega\neq\tilde{\epsilon}$, so the electron transition between two molecular levels is weak, and then we can focus on the main resonance and the sideband resonance of the molecular levels. One sees that (1) the main resonance peaks emerge at $V_g=\pm\tilde{\epsilon}/2$, corresponding to the molecular level lining up with the chemical potential; (2) with the decrease of $\Delta E/T$, the height of the peak (denoted as I_0) increases. This means that the molecular state becomes gradually delocalized over both dots, leading to an increase of the transmission probability. I_0 vs $\Delta E/T$ is shown in the inset of Fig. 3, and the curve varies as $J_0^2(\alpha)4\Gamma_{11}^L\Gamma_{11}^R/\Gamma_{11}^2=J_0^2(\alpha)/[1$

$+(\Delta E/2T)^2]$. As for the sideband resonance, i.e., the current value (denoted as I_1) at $V_g=\pm\tilde{\epsilon}/2\mp\omega$, we find that with $\Delta E/T$ decreasing, initially I_1 increases at large $\Delta E/T$, then decreases, which is different from the monotonic increasing of I_0 (see the inset of Fig. 3). This can be understood as follows: qualitatively, we have $I_1\sim J_1^2(\alpha)4\Gamma_{11}^L\Gamma_{11}^R/\Gamma_{11}^2$ with $\alpha=V_{ac}\Delta E/\omega\tilde{\epsilon}$. At the weak-coupling case (i.e., large $\Delta E/T$), α is almost a constant and I_1 is determined by the delocalized molecular level, leading to an increase of I_1 similar to I_0. However, when $\Delta E/T$ is small (the strong-coupling case), α decreases with $\Delta E/T$ decreasing, leading to a strong suppression of the sideband resonance of the molecular level.

Finally, we investigate the Rabi oscillations in the quantum-dot molecule. In the weak-coupling case, Stafford and Wingreen[6] found the Rabi splitting $\Omega_R\approx 2TJ_n(\alpha)$ for n-photon processes and the pumping current is a maximum when $\Omega_R=\Gamma$. We have reproduced their result in the weak-coupling case. The right inset of Fig. 2 shows $d\langle I\rangle/d\mu_L$ vs the chemical potential μ_L at $\omega=\tilde{\epsilon}$, where we see that the one photon resonant peak is split into two peaks with the separation of $2TJ_1(\alpha)$ due to the Rabi oscillations between one state and a photon sideband of the other state. But in the strong-coupling case, the Rabi oscillations are quite complicated; a bare state of one dot will be coupled with a series of sidebands of the bare state of the other dot because of the large coupling T. From the right inset of Fig. 2 (solid curve), we see that the one photon peak is split into four peaks with larger splitting of approximate 2γ and a smaller splitting of about $\gamma^2/4\omega$ (here $\Delta E\ll\tilde{\epsilon}$, i.e., $\alpha\approx 0$; and $\gamma\ll 2\omega$). In fact, the larger splitting is from the coupling $\gamma e^{-i\omega t}\tilde{c}_1^\dagger\tilde{c}_2+\text{H.c.}$ between the two molecular levels and the smaller splitting is from $\gamma e^{+i\omega t}\tilde{c}_1^\dagger\tilde{c}_2+\text{H.c.}$ [see Eq.(3)]. As in Ref. 6, we now investigate the resonant current $\langle I\rangle_{res}$ (for $\omega=\tilde{\epsilon}$) in the strong-coupling case. For $\mu_L-\epsilon_1,\epsilon_2-\mu_R\gg\Gamma$, and weak driving $V_{ac}\ll\omega$ (following $\gamma\ll\omega$), one has $\langle I\rangle_{res}=2e\Gamma\gamma^2/(4\gamma^2+\Gamma^2/4)$, in which $\langle I\rangle_{res}$ is maximum when $2\gamma=\Gamma/2$.

In conclusion, electron tunneling through a quantum-dot molecule under MW irradiation has been investigated. Both the weak-coupling and the strong-coupling cases as well as the crossover between them are studied in detail. Our results for both cases are in excellent agreement with the recent experiment by Oosterkamp *et al.* In addition, we show new features that can be verified experimentally. In particular, for the strong-coupling case we find that the heights of the photon-electron pumping current at zero bias rise much faster than $J_n^2(\alpha)$, with a different α, $\alpha=V_{ac}\Delta E/\omega\tilde{\epsilon}$, and that there is a strong suppression of the sideband resonance of the molecular level in the linear bias regime. An additional Rabi splitting in the strong coupling case is also found. Finally, the delocalizing behavior of the molecular levels as the coupling strength crosses over from the weak- to strong-coupling regime is predicted.

We gratefully acknowledge the financial support by a RGC grant from the HKSAR under Grant No. HKU 7112/97P, and a grant from the Chinese National Natural Science Foundation. We also thank Professor K. MacKeown for a critical reading of the manuscript.

[1] T. H. Oosterkamp *et al.*, Nature (London) **395**, 873 (1998).
[2] H. Drexler *et al.*, Appl. Phys. Lett. **67**, 2816 (1995).
[3] R. H. Blick *et al.*, Phys. Rev. Lett. **80**, 4032 (1998); Appl. Phys. Lett. **67**, 3924 (1995).
[4] C. Livermore, *et al.*, Science **274**, 1332 (1996).
[5] G. Schedelbeck *et al.*, Science **278**, 1792 (1997).
[6] C. A. Stafford and N. S. Wingreen, Phys. Rev. Lett. **76**, 1916 (1996).
[7] T. Ivanov, Phys. Rev. B **56**, 12 339 (1997).
[8] T. H. Stoof and Yu. V. Nazarov, Phys. Rev. B **53**, 1050 (1996).
[9] P. K. Tien and J. P. Gordon, Phys. Rev. **129**, 647 (1963).
[10] J. Iñarrea, G. Platero, and C. Tejedor, Phys. Rev. B **50**, 4581 (1994).
[11] Other interesting issues such as the influence of the electron's phase (Ref. 12) will be discussed in the future.
[12] A.P. Jauho and N.S. Wingreen, Phys. Rev. B **58**, 9619 (1998).
[13] N.S. Wingreen, A.-P. Jauho, and Y. Meir, Phys. Rev. B **48**, 8487 (1993); A.-P. Jauho, N.S. Wingreen, and Y. Meir, Phys. Rev. B **50**, 5528 (1994).
[14] Q.-f. Sun, J. Wang, and T.-h. Lin, Phys. Rev. B **58**, 13 007 (1998).
[15] C. Bruder and H. Schoeller, Phys. Rev. Lett. **72**, 1076 (1994).
[16] N.S. Wingreen, K.W. Jacobsen, and J.W. Wilkins, Phys. Rev. B **40**, 11 834 (1989).
[17] J.C. Cuevas, A.M.-Rodero, and A.L. Yeyati, Phys. Rev. B **54**, 7366 (1996).
[18] In deriving Eq. (6), we have used the same approximation as in Eq. (29) of Q.-f. Sun, J. Wang, and T.-h. Lin, Phys. Rev. B **59**, 13 126 (1999).
[19] In the assumption of $V_{gl}=V_{gr}\equiv V_g$, varying V_g is equivalent to shifting the uncoupled energy levels ϵ_l^0 and ϵ_r^0 keeping ΔE constant, since $\epsilon_l^0+\epsilon_r^0=0$ by assumption. In other words, it is equivalent to moving μ_L and μ_R in opposite directions.